LAWRENCE
LIVERMORE
NATIONAL
LABORATORY

UCRL-TR-235193

3H(d,n)4He S-factor from Ab Initio Overlap Functions

navratil1, thompson97, ormand1

October 2, 2007

Disclaimer

This work performed under the auspices of the U.S. Department of Energy by Lawrence Livermore National Laboratory under Contract DE-AC52-07NA27344.

^{3}H(d,n)^{4}He S-factor from *ab initio* overlap functions

Petr Navrátil, Ian Thompson and W. Erich Ormand*

Lawrence Livermore National Laboratory,

P.O. Box 808, L-414, Livermore, CA 94551, USA

(Dated: September 12, 2007)

Abstract

We present coupled channel calculations of the S-factor of ^{3}H(d,n)^{4}He transfer reaction. Potentials between different subclusters relevant for description of the transfer reaction are obtained by fits to cluster overlap functions calculated within the *ab initio* no-core shell model. This type of combined *ab initio*/potential model approach was successfully applied in the past to describe low-energy capture reactions important for nuclear astrophysics. For those reactions, typically a single or just a few channels were needed for an accurate description of the S-factor. For the ^{3}H(d,n)^{4}He transfer reaction, many channels are relevant, which makes the application of the combined approach quite challenging. In this report, we briefly outline the formalism, give overview of the capture reaction results obtained in the past, present in detail the calculations performed for the ^{3}H(d,n)^{4}He transfer reaction and give outlook for a full *ab initio* approach with predictive power capable to describe ^{3}H(d,n)^{4}He transfer reaction without ambiguities due to adjustable parameters.

PACS numbers:

*navratil1@llnl.gov

I. INTRODUCTION

Nuclear reactions occurring in a hot thermal environments are important to studies in astrophysics, energy, and national security. Of particular importance is the d(T,n)^{4}He reaction. Indeed, the reliable modeling of processes dependent on this reaction require an accurate evaluation of the reaction rate. While experimental data are preferable, it is very difficult to perform experiments at the lowest incident energies, which are often important for the modeling process. The reason for this is that because of the Coulomb barrier, the reaction rate decreases substantially with incident energy, and experiments are limited by background. Thus, an extrapolation method is required. It is important to note, however, that it is dangerous to perform an extrapolation based entirely on current experimental data. This is primarily because data at low energies have larger uncertainties that can mask the presence of resonances or the effects of coupling to other channels in the reaction. This is illustrated in Fig. 1 for the d(T,n)^{4}He reaction where two extrapolations for the S-factor based on an R-matrix fit to existing data are shown [1]. Here, the fit labeled "Livermore" included only the large resonance at roughly 50 keV, while the fit labeled "Los Alamos" included coupling to other channels in the reaction. When these other couplings are included, the S-factor increases, and roughly a 5% discrepancy in the S-factor at low energies. This can affect modeling of systems at low temperatures.

It should be noted that the R-matrix is not a theory for the process, but really is not much more than a framework to perform a fit to the data. In this regard, a more fundamental theory for reactions involving light nuclei is needed. In fact, at this point, no fundamental theory for light-ion reactions exists. At LLNL, the Nuclear theory & Modeling (NTM) Group has active research in the *ab initio* description of light nuclei, and is extending this effort to describe dynamic processes, such as reactions. In this report, we show the results of our first-generation model, which while it is not fully *ab initio*, is based on the structure obtained with the *ab initio*, No-core Shell Model (NCSM). We use the NCSM to compute radial-cluster overlaps that are used to describe the radial wave functions for the cluster channels. Since one of the weaknesses of the NCSM is the asymptotic behavior of the radial wave functions and the inclusion of continuum states, we use a potential model to describe the dynamics within a coupled-channels framework. While this framework was very successful for the radiative capture reaction ^{7}Be(p,γ)^{8}B, our results point to some deficiencies in this

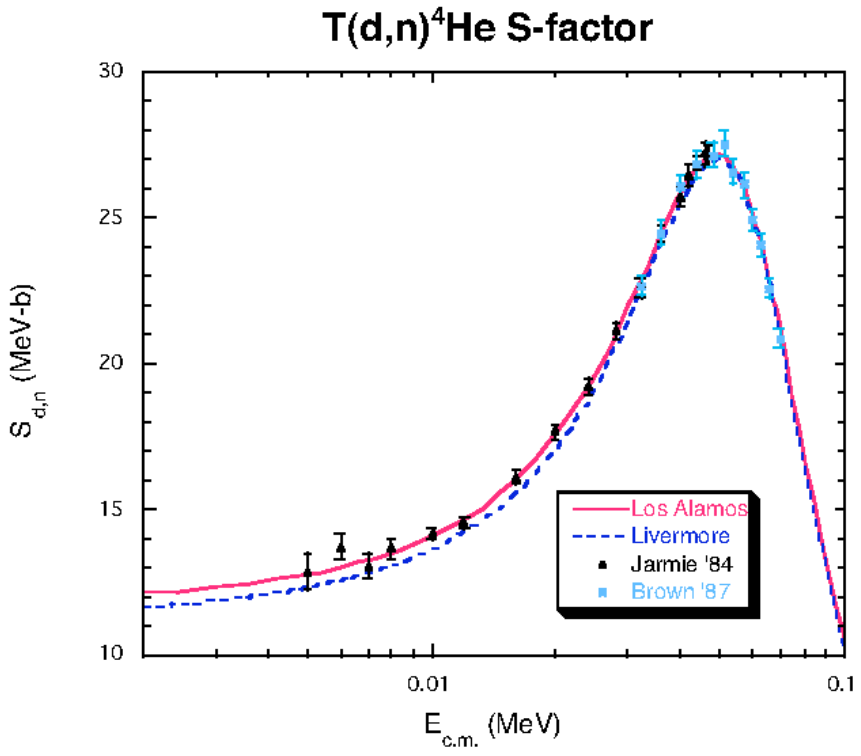

FIG. 1: Extrapolation of the ^{3}H(d,n)^{4}He S-factor to very low energies.

approach due to a significantly increased complexity of the d(T,n)^{4}He reaction, in particular its multi-channel character, and the need to finalize a fully *ab initio* picture based on the resonating group method (RGM), which is currently underway in the NTM group.

This report is organized as follows. In Sect. II, we briefly introduce the *ab initio* NCSM. In Sect. 3, we discuss the calculation of the overlap functions from the *ab initio* NCSM wave functions, the correction of their asymptotic behavior using the Woods-Saxon potential fit and present the past successful applications of the corrected overlap functions to capture reactions important for astrohysics: the ^{7}Be(p,γ)^{8}B and ^{3}He(α,γ)^{7}Be. Success of those applications served as a motivation to generalize the approach and use it for the far more complex case of the ^{3}H(d,n)^{4}He transfer reaction. In Sect. IV, we discuss the calculation of the ^{3}H(d,n)^{4}He S-factor within the combined *ab initio* NCSM/potential model approach. Conclusions are presented in Sect. V and in Sect. VI we give an outlook of our work in

progress, a fully *ab initio* calculation of the light-ion reactions using a combination of the *ab initio* NCSM with the resonating group method technique.

II. *AB INITIO* NO-CORE SHELL MODEL

In the NCSM, we start from the intrinsic A-nucleon Hamiltonian $H_A = T_{rel} + \mathcal{V}$, where T_{rel} is the relative kinetic energy and $\mathcal{V}$ is the sum of two-body or possibly higher-body nuclear and Coulomb interactions. To facilitate our calculations, we add a center-of-mass Harmonic Oscillator (HO) Hamiltonian, whose effect will be eventually subtracted in the final many-body calculation, and for a two-body interaction obtain the HO frequency-dependent Hamiltonian $H_A^\Omega = \sum_i^A h_i + \sum_{i<j}^A V_{ij}^{\Omega,A}$. The h_i is a one-body HO term and the two-body interaction $V_{ij}^{\Omega,A}$ contains a term proportional to $\frac{1}{A}(\vec{r}_i - \vec{r}_j)^2$ [2–4]. Since we solve the many-body problem in a finite HO basis space, it is necessary that we derive a model-space dependent effective Hamiltonian. For this purpose, we perform a unitary transformation [5, 6] on the Hamiltonian, which accommodates the short-range correlations. In general, the transformed Hamiltonian is an A-body operator. The first-order approximation is to develop a two-particle cluster effective Hamiltonian, while the next improvement is to include three-particle clusters, and so on. The effective interaction is obtained from the decoupling condition between the model space and the excluded space for the two- or three-nucleon transformed Hamiltonian. On the two-body cluster level, we solve $h_1 + h_2 + V_{12}^{\Omega,A}$, and from the transformation we obtain $V_{2-\mathrm{eff},12}^{\Omega,A}$ and then solve the A-body problem using $\sum_i^A h_i + \sum_{i<j}^A V_{2-\mathrm{eff},ij}^{\Omega,A}$. On the three-body cluster level, we solve $h_1 + h_2 + h_3 + V_{12}^{\Omega,A} + V_{13}^{\Omega,A} + V_{23}^{\Omega,A}$ to obtain $V_{3-\mathrm{eff},123}^{\Omega,A}$, and then use $\sum_i^A h_i + \frac{1}{A-2}\sum_{i<j<k}^A V_{3-\mathrm{eff},ijk}^{\Omega,A}$ for the A-body problem. The resulting two- or three-body effective Hamiltonian depends on the nucleon number A, the HO frequency Ω, and $N_{\max}$. The effective interaction approaches the bare interaction for $N_{\max} \to \infty$.

III. CLUSTER OVERLAP FUNCTIONS AND S-FACTORS OF CAPTURE REACTIONS

In the *ab initio* NCSM calculations, we are able to obtain wave functions low-lying states of light nuclei in large model spaces. An interesting and important question is, what is the cluster structure of these wave functions. That is we want to understand, how much,

e.g. an ^{6}Li eigenstate looks like ^{4}He plus deuteron, an ^{7}Be eigenstate looks like ^{4}He plus ^{3}He, an ^{8}B eigenstate looks like ^{7}Be plus proton and so on. This information is important for the description of low-energy nuclear reactions. To gain insight, one introduces channel cluster form factors (or overlap integrals, overlap functions). The formalism for calculating the channel cluster form factors from the NCSM wave functions was developed in Ref. [7]. Here we just briefly repeat a part of the formalism relevant to the simplest case when the lighter of the two clusters is a single-nucleon.

We consider a composite system of A nucleons, i.e. ^{8}B, a nucleon projectile, here a proton, and an $A-1$-nucleon target, i.e. ^{7}Be. Both nuclei are assumed to be described by eigenstates of the NCSM effective Hamiltonians expanded in the HO basis with identical HO frequency and definitions of the model space that are the same (for the eigenstates of the same parity) or differing by one unit of the HO excitation (for the eigenstates of opposite parity). The target and the composite system is described by wave functions expanded in Slater determinant single-particle HO basis (that is obtained from a calculation using a shell model code like Antoine).

Let us introduce a projectile-target wave function

$$\begin{aligned}\langle\vec{\xi}_1\ldots\vec{\xi}_{A-2}r'\hat{r}|\Phi^{(A-1,1)JM}_{(l\frac{1}{2})j;\alpha I_1}; \delta_r\rangle \;=\; &\sum (jmI_1M_1|JM)(lm_l\tfrac{1}{2}m_s|jm)\tfrac{\delta(r-r')}{rr'} \\ &\times Y_{lm_l}(\hat{r})\chi_{m_s}\langle\vec{\xi}_1\ldots\vec{\xi}_{A-2}|A-1\alpha I_1M_1\rangle \;, \end{aligned} \tag{1}$$

where $\langle\vec{\xi}_1\ldots\vec{\xi}_{A-2}|A-1\alpha I_1M_1\rangle$ and χ_{m_s} are the target and the nucleon wave function, respectively. Here, l is the channel relative orbital angular momentum, $\vec{\xi}$ are the target Jacobi coordinates defined by

$$\vec{\xi}_0 \;=\; \sqrt{\frac{1}{A}}\left[\vec{r}_1+\vec{r}_2+\ldots+\vec{r}_A\right] \;, \tag{2}$$

$$\vec{\xi}_1 \;=\; \sqrt{\frac{1}{2}}\left[\vec{r}_1-\vec{r}_2\right] \;, \tag{3}$$

$$\vec{\xi}_2 \;=\; \sqrt{\frac{2}{3}}\left[\frac{1}{2}\left(\vec{r}_1+\vec{r}_2\right)-\vec{r}_3\right] \;, \tag{4}$$

$$\ldots$$

$$\vec{\xi}_{A-2} \;=\; \sqrt{\frac{A-2}{A-1}}\left[\frac{1}{A-2}\left(\vec{r}_1+\vec{r}_2+\ldots+\vec{r}_{A-2}\right)-\vec{r}_{A-1}\right] \;, \tag{5}$$

$$\vec{\xi}_{A-1} \;=\; \sqrt{\frac{A-1}{A}}\left[\frac{1}{A-1}\left(\vec{r}_1+\vec{r}_2+\ldots+\vec{r}_{A-1}\right)-\vec{r}_A\right] \;, \tag{6}$$

and $\vec{r}=\left[\frac{1}{A-1}\left(\vec{r}_1+\vec{r}_2+\ldots+\vec{r}_{A-1}\right)-\vec{r}_A\right]$ describes the relative distance between the nucleon

and the center of mass of the target. The spin and isospin coordinates within the target were omitted for simplicity.

The channel cluster form factor is then defined by

$$g^{A\lambda J}_{(l\frac{1}{2})j;A-1\alpha I_1}(r) = \langle A\lambda J|\mathcal{A}\Phi^{(A-1,1)J}_{(l\frac{1}{2})j;\alpha I_1};\delta_r\rangle \ , \tag{7}$$

with $\mathcal{A}$ the antisymmetrizer and $|A\lambda J\rangle$ an eigenstate of the A-nucleon composite system (here ^{8}B). It can be calculated from the NCSM eigenstates obtained in the Slater-determinant basis from a reduced matrix element of the creation operator. It can be derived as follows. First, we use the factorization of the translationally-invariant NCSM Hamiltonian eiegenstates

$$\begin{aligned} &\langle\vec{r}_1\ldots\vec{r}_A\sigma_1\ldots\sigma_A\tau_1\ldots\tau_A|A\lambda JMTM_T\rangle_{\rm SD} \\ =\ &\langle\vec{\xi}_1\ldots\vec{\xi}_{A-1}\sigma_1\ldots\sigma_A\tau_1\ldots\tau_A|A\lambda JMTM_T\rangle\varphi_{000}(\vec{\xi}_0;b) \ , \end{aligned} \tag{8}$$

for both the composite A-nucleon and the target $A-1$-nucleon eigenstate. With the help of the HO wave function transformations

$$\begin{aligned} &\sum_{Mm}(LMlm|Qq)\varphi_{NLM}(\vec{R}^{A-1}_{\rm CM})\varphi_{nlm}(\vec{r}_A) = \\ &\sum_{n'l'm'N'L'M'}\langle n'l'N'L'Q|NLnlQ\rangle_{\frac{1}{A-1}}(l'm'L'M'|Qq)\varphi_{n'l'm'}(\vec{\xi}_{A-1})\varphi_{N'L'M'}(\vec{\xi}_0) \ , \end{aligned} \tag{9}$$

we obtain

$${}_{\rm SD}\langle A\lambda J|\mathcal{A}\Phi^{(A-1,1)J}_{(l\frac{1}{2})j;\alpha I_1};nl\rangle_{\rm SD} \ = \langle nl00l|00nll\rangle_{\frac{1}{A-1}}\ \langle A\lambda J|\mathcal{A}\Phi^{(A-1,1)J}_{(l\frac{1}{2})j;\alpha I_1};nl\rangle \ , \tag{10}$$

with a general HO bracket due to the CM motion. The nl in (10) refers to a replacement of δ_r by the HO $R_{nl}(r)$ radial wave function. Second, we relate the SD overlap to a linear combination of matrix elements of a creation operator between the target and the composite eigenstates ${}_{\rm SD}\langle A\lambda J|a^\dagger_{nlj}|A-1\alpha I_1\rangle_{\rm SD}$. The subscript SD refers to the fact that these states were obtained in the Slater determinant basis. Such matrix elements are easily calculated by shell model codes. The result is

$$\begin{aligned} \langle A\lambda J|\mathcal{A}\Phi^{(A-1,1)J}_{(l\frac{1}{2},j);\alpha I_1};\delta_r\rangle \ =\ &\sum_n R_{nl}(r)\frac{1}{\langle nl00l|00nll\rangle_{\frac{1}{A-1}}}\frac{1}{\hat{J}}(-1)^{I_1-J-j} \\ &\times\ {}_{\rm SD}\langle A\lambda J||a^\dagger_{nlj}||A-1\alpha I_1\rangle_{\rm SD} \ . \end{aligned} \tag{11}$$

The eigenstates expanded in the Slater determinant basis contain CM components. A general HO bracket, which value is simply given by

$$\langle nl00l|00nll\rangle_{\frac{1}{A-1}} = (-1)^l \left(\frac{A-1}{A}\right)^{\frac{2n+l}{2}} , \tag{12}$$

then appears in Eq. (11) in order to remove these components. The $R_{nl}(r)$ in Eq. (11) is the radial HO wave function with the oscillator length parameter $b = \sqrt{\frac{\hbar}{\frac{A-1}{A}m\Omega}}$, where m is the nucleon mass.

A conventional spectroscopic factor is obtained by integrating the square of the cluster form factor:

$$S^{A\lambda J}_{(l\frac{1}{2})j;A-1\alpha I_1} = \int dr r^2 |g^{A\lambda J}_{(l\frac{1}{2})j;A-1\alpha I_1}(r)|^2 . \tag{13}$$

A generalization for projectiles (= the lighter of the two clusters) with 2, 3 or 4 nucleons is straightforward, although the expressions become more involved. In all cases, the projectile is described by wave function expanded in Jacobi coordinate HO basis, while the composite and the target eigenstates are expanded in the Slater determinant HO basis. Full details are given in Ref. [7].

The overlap functions introduced in this subsection are relevant for description of low-energy nuclear reactions. Before we procceed to the application to the ^{3}H(d,n)^{4}He S-factor, we first briefly review the past applications of the *ab initio* overlap functions to γ-capture reactions important for nuclear astrophysics. Success of those applications served as a motivation to generalize the approach and use it for the more complex case of the ^{3}H(d,n)^{4}He transfer reaction.

A. ^{7}Be(p,γ)^{8}B

The ^{7}Be(p,γ)^{8}B capture reaction serves as an important input for understanding the solar neutrino flux [9]. Recent experiments have determined the neutrino flux emitted from ^{8}B with a precision of 9% [10]. On the other hand, theoretical predictions have uncertainties of the order of 20% [11, 12]. The theoretical neutrino flux depends on the ^{7}Be(p,γ)^{8}B S-factor. Many experimental and theoretical investigations studied this reaction.

In this ection, we discuss a calculation of the ^{7}Be(p,γ)^{8}B S-factor starting from *ab initio* wave functions of ^{8}B and ^{7}Be. We note that full details of our ^{7}Be(p,γ)^{8}B investigation were published in Refs. [14, 15].

Our calculations for both ^{7}Be and ^{8}B nuclei were performed using the high-precision CD-Bonn 2000 NN potential [8] in model spaces up to $10\hbar\Omega$ ($N_{\max} = 10$) for a wide range of HO frequencies. From the obtained ^{8}B and ^{7}Be wave functions, we calculate the channel cluster form factors (overlap functions, overlap integrals) $g^{A\lambda J}_{(l\frac{1}{2})j;A-1\alpha I_1}(r)$ as discussed in the previous subsection. Here, $A = 8$, l is the channel relative orbital angular momentum and $\vec{r} = \left[\frac{1}{A-1}\left(\vec{r}_1 + \vec{r}_2 + \ldots + \vec{r}_{A-1}\right) - \vec{r}_A\right]$ describes the relative distance between the proton and the center of mass of ^{7}Be. The two most important channels are the p-waves, $l = 1$, with the proton in the $j = 3/2$ and $j = 1/2$ states, $\vec{j} = \vec{l} + \vec{s}$, $s = 1/2$. In these channels, we obtain the spectroscopic factors of 0.96 and 0.10, respectively. The dominant $j = 3/2$ overlap integral is presented in the left panel of Fig. 2 by the full line. The $10\hbar\Omega$ model space and the HO frequency of $\hbar\Omega = 12$ MeV were used. Despite the fact, that a very large basis was employed in the present calculation, it is apparent that the overlap function is nearly zero at about 10 fm. This is a consequence of the HO basis asymptotic behavior. As already discussed, in the *ab initio* NCSM, the short-range correlations are taken into account by means of the effective interaction. The medium-range correlations are then included by using a large, multi-$\hbar\Omega$ HO basis. The long-range behavior is not treated correctly, however. The proton capture on ^{7}Be to the weakly bound ground state of ^{8}B associated dominantly by the $E1$ radiation is a peripheral process. In order to calculate the S-factor of this process we need to go beyond the *ab initio* NCSM as done up to this point. We expect, however, that the interior part of the overlap function is realistic. It is then straightforward to find a quick fix and correct the asymptotic behavior of the overlap functions, which should be proportional to the Whittaker function.

One possibility we explored utilizes solutions of a Woods-Saxon (WS) potential, i.e.,

$$V^{\rm WS}(r) = V_0 f(r, R_0, a_0) - V_{ls}\left(\frac{\hbar}{m_\pi c}\right)\frac{1}{r}\frac{\rm d}{{\rm d}r} f(r, R_{ls}, a_{ls})\vec{l}\cdot\vec{s} + V_{Coul}(r, R_0)\ , \qquad (14)$$

with $f(r, R, a) = \frac{1}{1+\exp((r-R)/a)}$. In particular, we performed a least-square fit of a WS potential solution to the interior of the NCSM overlap in the range of $0 - 4$ fm. The WS potential parameters were varied in the fit under the constraint that the experimental separation energy of ^{7}Be+p, $E_0 = 0.137$ MeV, was reproduced. In this way we obtain a perfect fit to the interior of the overlap integral and a correct asymptotic behavior at the same time. The result is shown in Fig. 2 by the dashed line.

Another possibility is a direct matching of logarithmic derivatives of the NCSM overlap

integral and the Whittaker function: $\frac{d}{dr}ln(rg_{lj}(r)) = \frac{d}{dr}ln(C_{lj}W_{-\eta,l+1/2}(2k_0r))$, where η is the Sommerfeld parameter, $k_0 = \sqrt{2\mu E_0}/\hbar$ with μ the reduced mass and E_0 the separation energy. Since asymptotic normalization constant (ANC) C_{lj} cancels out, there is a unique solution at $r = R_m$. For the discussed overlap presented in Fig. 2, we found $R_m = 4.05$ fm. The corrected overlap using the Whittaker function matching is shown in Fig. 2 by a dotted line. In general, we observe that the approach using the WS fit leads to deviations from the original NCSM overlap starting at a smaller radius. In addition, the WS solution fit introduces an intermediate range from about 4 fm to about 6 fm, where the corrected overlap deviates from both the original NCSM overlap and the Whittaker function. Perhaps, this is a more realistic approach compared to the direct Whittaker function matching.

The S-factor for the reaction ^{7}Be(p, γ)^{8}B also depends on the continuum wave function, $R_{lj}^{(c)}$ that we obtain for s and d waves from a WS potential model. Since the largest part of the integrand stays outside the nuclear interior, one expects that the continuum wave functions are well described in this way. In order to have the same scattering wave function in all the calculations, we chose a WS potential from Ref. [16] that was fitted to reproduce the p-wave 1^+ resonance in ^{8}B. It was argued [17] that such a potential is also suitable for the description of s- and d-waves. We note that the S-factor is very weakly dependent on the choice of the scattering-state potential (using our fitted potential for the scattering state instead changes the S-factor by less than 1.5 eV b at 1.6 MeV with no change at 0 MeV).

Our obtained S-factor is presented in Figs. 3 where contribution from the two partial waves are shown together with the total result. It is interesting to note a good agreement of our calculated S-factor with the recent Seattle direct measurement [18].

In order to judge the convergence of our S-factor calculation, we performed a detailed investigation of the model-space-size and the HO frequency dependencies. We used the HO frequencies in the range from $\hbar\Omega = 11$ MeV to $\hbar\Omega = 15$ MeV and the model spaces from $6\hbar\Omega$ to $10\hbar\Omega$. By analysing these results, we arrived at the S-factor value of $S_{17}(10\,\mathrm{keV}) = 22.1 \pm 1.0$ eV b.

B. ^{3}He(α,γ)^{7}Be

The ^{3}He(α,γ)^{7}Be capture reaction cross section was identified the most important uncertainty in the solar model predictions of the neutrino fluxes in the p-p chain [12]. We

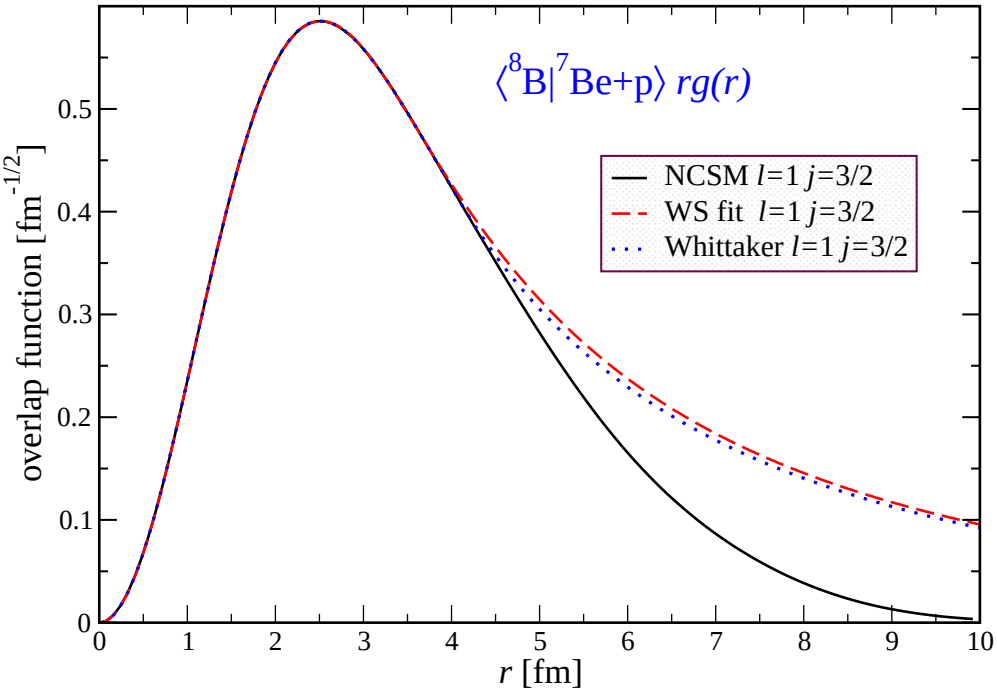

FIG. 2: Overlap function, $rg(r)$, for the ground state of ^{8}B with the ground state of ^{7}Be plus proton as a dependence on separation between the ^{7}Be and the proton. The p-wave channel with $j = 3/2$ is shown. The full line represents the NCSM result obtained using the CD-Bonn 2000 NN potential, the $10\hbar\Omega$ model space and the HO frequency of $\hbar\Omega = 12$ MeV. The dashed lines represent corrected overlaps obtained from a Woods-Saxon potential whose parameters were fit to the NCSM overlaps up to 4.0 fm under the constraint to reproduce the experimental separation energy. The dotted lines represent overlap corrections by the direct Whittaker function matching.

investigated the bound states of ^{7}Be, ^{3}He and ^{4}He within the *ab initio* NCSM and calculated the overlap functions of ^{7}Be bound states with the ground states of ^{3}He plus ^{4}He as a function of separation between the ^{3}He and the α particle. The obtained p-wave overlap functions of the ^{7}Be $3/2^-$ ground state excited state are presented in Fig. 4 by the full line. The dashed lines show the corrected overlap function obtained by the least-square fits of the WS parameters done in the same way as in the ^{8}B$\leftrightarrow^7$Be+p case. The corresponding NCSM spectroscopic factors obtained using the CD-Bonn 2000 in the $10\hbar\Omega$ model space for ^{7}Be ($12\hbar\Omega$ for ^{3,4}He) and HO frequency of $\hbar\Omega = 13$ MeV are 0.93 and 0.91 for the ground state

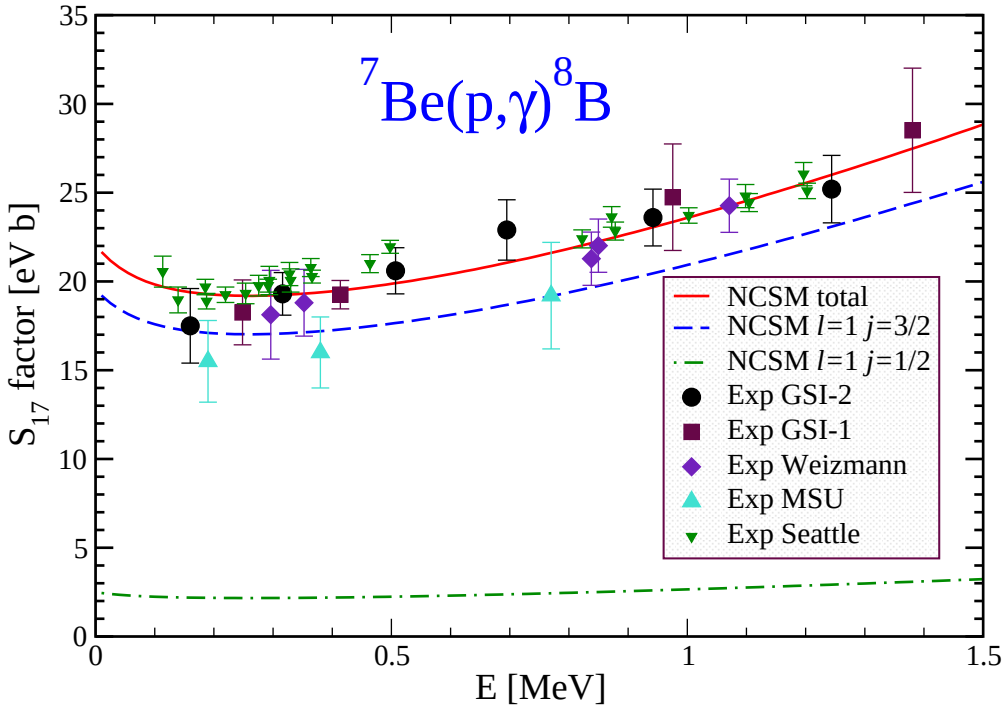

FIG. 3: The ^{7}Be(p,γ)^{8}B S-factor obtained using the NCSM overlap functions with corrected asymptotics as described in the text. The dashed and dashed-dotted lines show the contribution due to the $l = 1$, $j = 3/2$ and $j = 1/2$ partial waves, respectively. Experimental values are from Refs. [18, 19].

and the first excited state of ^{7}Be, respectively. We note that contrary to the ^{8}B$\leftrightarrow^7$Be+p case, the ^{7}Be$\leftrightarrow^3$He+α p-wave overlap functions have a node.

Using the corrected overlap functions and a ^{3}He+α scattering state obtained using the potential model of Ref. [20] we calculated the ^{3}He(α,γ)^{7}Be S-factor. Our $10\hbar\Omega$ result is presented in the left panel of Fig. 5. We show the total S-factor as well as the contributions from the capture to the ground state and the first excited state of ^{7}Be. By investigating the model space dependence for $8\hbar\Omega$ and $10\hbar\Omega$ spaces we estimate the ^{3}He(α,γ)^{7}Be S-factor at zero energy to be higher than 0.44 keV b, the value that we obtained in the discussed case shown in Fig. 5. Our results are similar to those obtained by K. Nollett [21] using the variational Monte Carlo wave functions for the bound states and potential model wave functions for the scattering state.

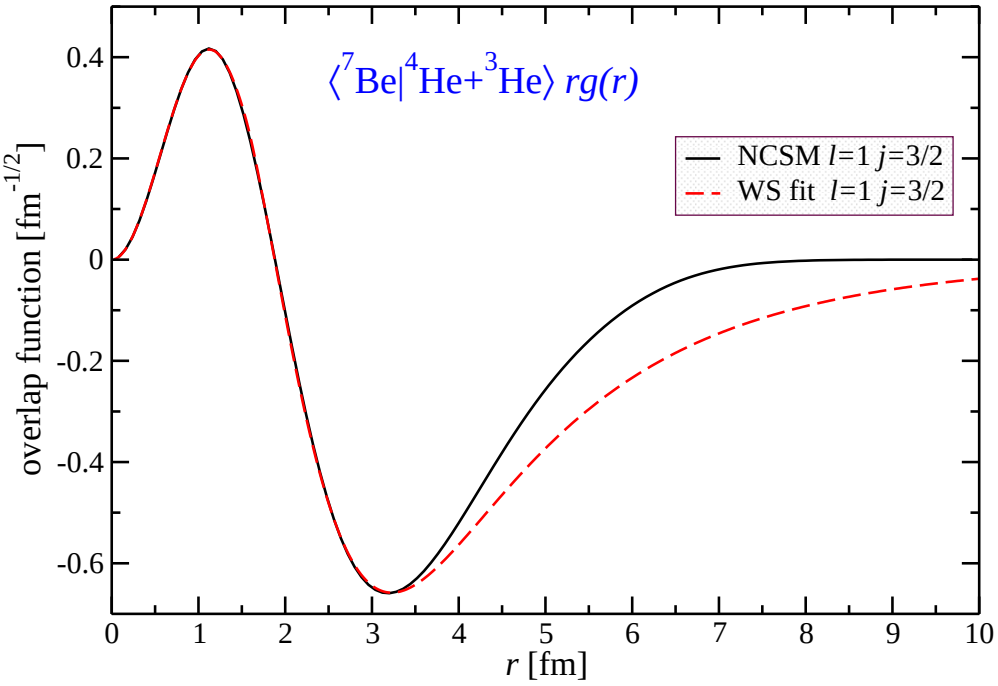

FIG. 4: The overlap function, $rg(r)$, for the first excited state of ^{7}Be with the ground state of ^{3}He plus α as a dependence on separation between the ^{3}He and the α particle. The p-wave channel overlap function with $j = 3/2$ is shown. The full line represents the NCSM result obtained using the CD-Bonn 2000 NN potential and the $10\hbar\Omega$ model space for ^{7}Be ($12\hbar\Omega$ for ^{3,4}He) with the HO frequency of $\hbar\Omega = 13$ MeV. The dashed line represents a corrected overlap obtained with a Woods-Saxon potential whose parameters were fit to the NCSM overlap up to 3.4 fm under the constraint to reproduce the experimental separation energy.

C. ^{3}H(α,γ)^{7}Li

An important check on the consistency of the ^{3}He(α,γ)^{7}Be S-factor calculation is the investigation of the mirror reaction ^{3}H(α,γ)^{7}Li, for which more accurate data exist [22]. Our results obtained using the CD-Bonn 2000 NN potential are shown in Fig. 6. It is apparent that our ^{3}H(α,γ)^{7}Li results are consistent with our ^{3}He(α,γ)^{7}Be calculation. We are on the lower side of the data and we find an increase of the S-factor as we increase the size of our basis.

More details on the *ab initio* NCSM investigation of the ^{3}He(α,γ)^{7}Be and ^{3}H(α,γ)^{7}Li

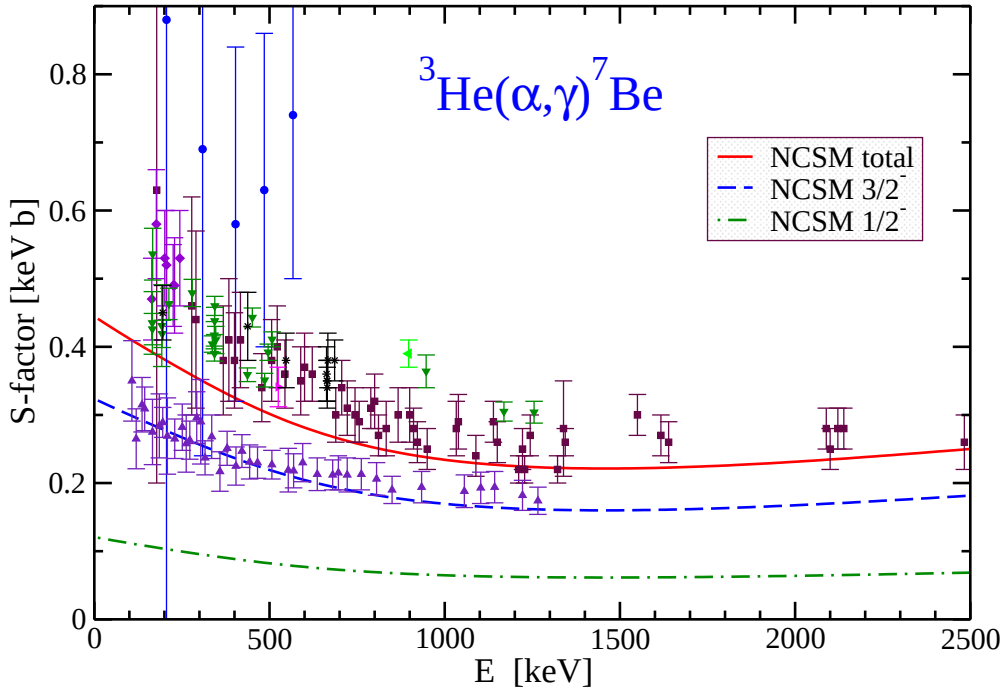

FIG. 5: The full line shows the ^{3}He(α,γ)^{7}Be S-factor obtained using the NCSM overlap functions with corrected asymptotics. The dashed lines show the ^{7}Be ground- and the first excited state contributions. The calculation was done using the CD-Bonn 2000 NN potential and the $10\hbar\Omega$ model space for ^{7}Be ($12\hbar\Omega$ for ^{3,4}He) with the HO frequency of $\hbar\Omega = 13$ MeV.

S-factors are given in Ref. [23].

IV. CALCULATION OF THE ^{3}H(D,N)^{4}HE S-FACTOR

Based on the success of the capture reactions S-factor calculations starting from the *ab initio* NCSM overlap functions, we now want to generalize this approach to the more complex calculation of the ^{3}H(d,n)^{4}He S-factor. In this case, there are several different channels that need to be taken into account but, most importantly, the reaction proceeds through a $3/2^+$ resonance in ^{5}He unlike the capure reactions discussed earlier that proceeded through a non-resonant E1 capture. Our task is not just to determine the cluster-cluster potentials that describe the bound states but also potentials that describe resonances in ^{5}He. On top of it, those potentials should describe the system at the resonant energy but also at different

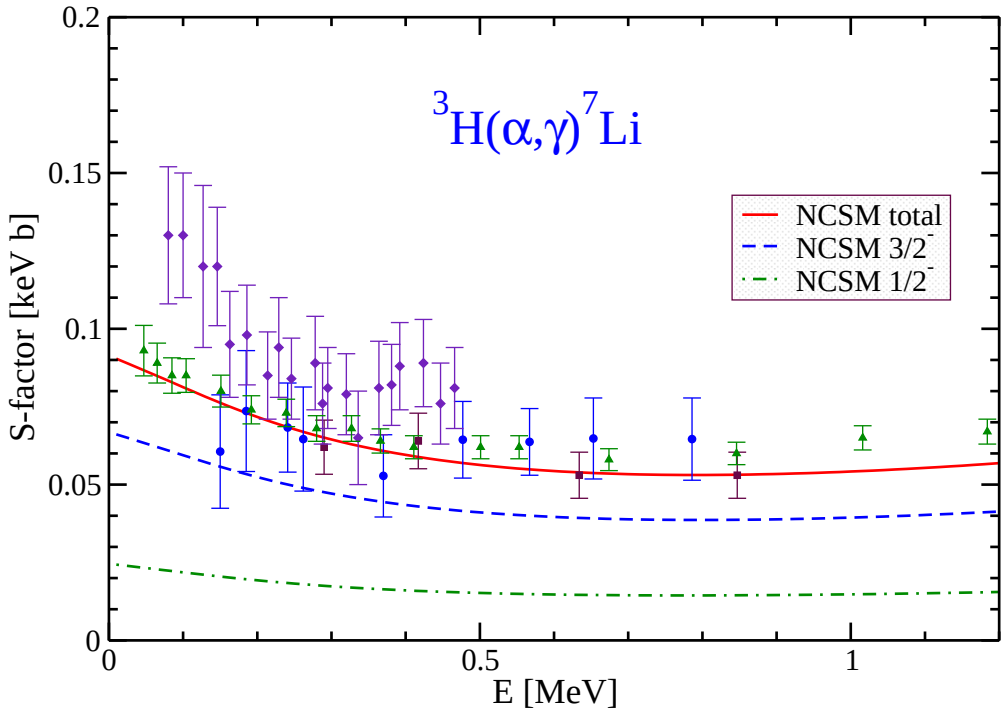

FIG. 6: The full line shows the ^{3}H(α,γ)^{7}Li S-factor obtained using the NCSM overlap functions with corrected asymptotics. The dashed lines show the ^{7}Li ground- and the first excited state contributions. The calculation was done using the CD-Bonn 2000 NN potential and the 10$\hbar\Omega$ model space for ^{7}Li (12$\hbar\Omega$ for ^{3}H and ^{4}He) with the HO frequency of $\hbar\Omega = 13$ MeV.

energies in some energy range that includes the resonant energy.

We perform our calculations in a coupled channel formalism using the code Fresco. We assume that the reaction proceeds as a transfer reaction when the deuteron is broken and the proton is attached to the ^{3}H nucleus. In addition, we consider a process in which the triton is broken into the deuteron and a neutron and the two deuterons merge to form ^{4}He. In order to set up the coupled channel equations, we need to determine potentials between different cluster partitions. In particular, we need to consider the following partitions and cluster overlap functions for the bound states: ^{3}H$\leftrightarrow^2$H+n, ^{4}eH$\leftrightarrow^2$H+d, ^{4}eH$\leftrightarrow^3$H+p,and also we need to input a nucleon-nucleon potential to obtain the deuteron wave function. Then, we need to know the n+^{4}He scattering potential that we obtain from fitting the *ab initio* NCSM $3/2^-$ ^{5}He wave function at the experimental resonance energy and finally and most

importantly, we need to determine the d+t scattering potential that we determine by fitting the *ab initio* NCSM $3/2^+$ ^{5}He wave function at the experimental resonance energy.

In the following subsections we first desribe the potential determination for the bound states and in next for the scattering states.

A. Bound-state potentials from *ab initio* wave functions

First, we investigate the overlap function of ^{3}H bound state with d+n to dermine a potential that binds deuteron and neutron to form ^{3}H. In Fig. 7, we show the overlap function obtained within the *ab initio* NCSM by a black line. The dashed red line then shows our WS potential fit to the interior part of the oveelap function under the constraint to reproduce the experimental separation energy of 6.257 MeV. The WS parameters and the spectroscopic factor are given in Table I.

TABLE I: Parameters of the Woods-Saxon potentials obtained in the fits to the interior part of the NCSM bound-state overlap functions under the constraint to reproduce experimental separation energies. The spectroscopic factors are given in the last column.

	V_0	R_0	a_0	S
$\langle^3$H$\vert^2$H+n$\rangle$	-34.541	2.207	0.436	1.321
$\langle^4$He$\vert$d+d$\rangle$	-63.963	1.941	0.550	0.936
$\langle^4$He$\vert^3$H+p$\rangle$	-53.788	2.264	0.417	1.719

Next, we consider the overlap function of ^{4}He with d+d to dermine a potential that binds the two deuterons to form ^{4}He. Our *ab initio* NCSM overlap function is presented in Fig. 8 by the solid black line. The WS fit to the interior part of the overlap is shown by the red dashed line. The experimental separation energy of 23.846 MeV was used as a constraint. Unlike in the cases of the previously studied overlap functions, due to the fact that ^{4}He is so deeply bound there is a very little visible difference even at the tail of the overlap function.

In Fig. 9, we present the overlap function of ^{4}He with ^{3}H and proton. The *ab initio* NCSM overlap function is given by the solid black line while the WS fit to the interior of the *ab initio* overlap is shown by the red dashed line. The fit was constrained by the experimental separation energy of 19.814 MeV. Similarly as in the case of the ^{4}He$\leftrightarrow$d+d overlap function,

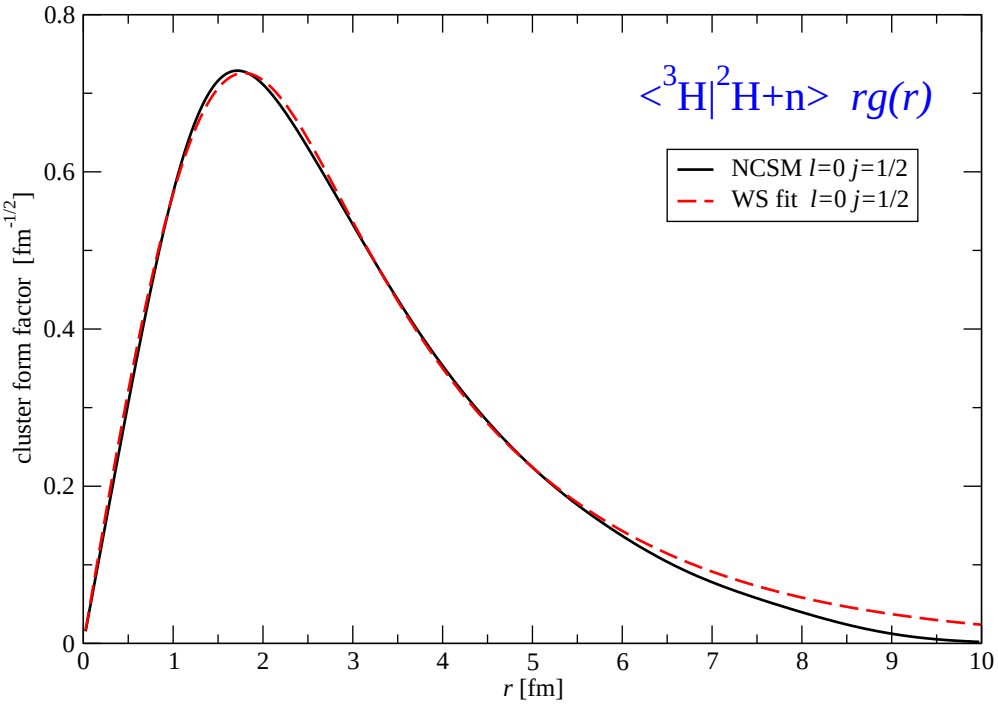

FIG. 7: Overlap function, $rg(r)$, for the ground state of ^{3}H with the deuteron plus proton as a dependence of their separation. The s-wave channel with $j = 1/2$ is shown. The full line represents the NCSM result obtained using the CD-Bonn 2000 NN potential, the $18\hbar\Omega$ model space and the HO frequency of $\hbar\Omega = 28$ MeV. The dashed lines represent corrected overlaps obtained from a Woods-Saxon potential whose parameters were fit to the NCSM overlap up to 5.0 fm under the constraint to reproduce the experimental separation energy.

there is little visible difference between the *ab initio* and the fitted overlap even in the tail region due to the large separation energy of ^{3}H+p in ^{4}He. The constrained fit gives us a WS potential that binds the ^{3}H and proton to form ^{4}He. This potential together with the spectroscopic factor obtained in our *ab initio* calculation serves as input for the coupled channel calculations of the ^{3}H(d,n)^{4}He S-factor. The WS parameters and the spectroscopic factors can be found in Table I.

We also need to input a nucleon-nucleon potential to obtain the deuteron wave function. For this purpose we employ the Reid soft-core potential that is already built into the Fresco code.

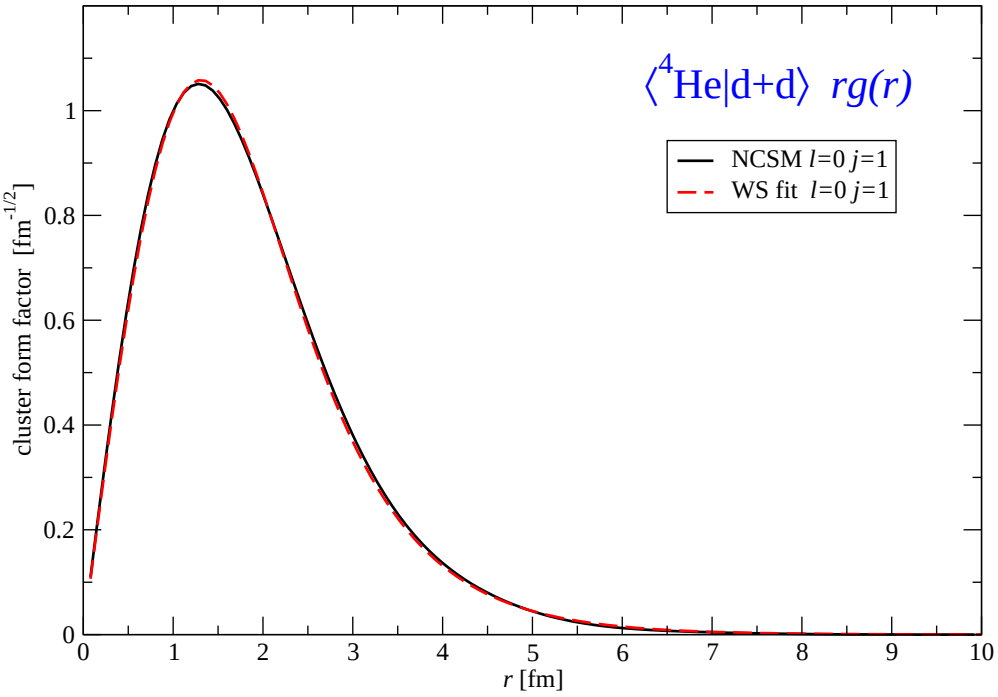

FIG. 8: Overlap function, $rg(r)$, for the ground state of ^{4}He with the deuteron plus deuteron as a dependence of their separation. The s-wave channel with $j = 1$ is shown. The full line represents the NCSM result obtained using the CD-Bonn 2000 NN potential, the $12\hbar\Omega$ model space and the HO frequency of $\hbar\Omega = 19$ MeV. The dashed lines represent corrected overlaps obtained from a Woods-Saxon potential whose parameters were fit to the NCSM overlap up to 4.0 fm under the constraint to reproduce the experimental separation energy.

B. n+^{4}He scattering potential from the ^{5}He $3/2^-$ resonance *ab initio* wave function

To calculate the ^{3}H(d,n)^{4}He S-factor, we need to determine in addition to the cluster-cluster binding potentials also the scattering potentials that describe the incoming and outgoing binary systems. We first start with the simpler case of the n+^{4}He. The ^{3}H(d,n)^{4}He reaction proceeds primarily through a $3/2^+$ resonance. Therefore, it is important to know the n+^{4}He potenatial that describe well particularly the $d3/2$ channel. Experimentally, it is known that the n+^{4}He phase shift is very small in this channel. At the same time, the n+^{4}He scattering is dominated by the $p3/2$ resonance corresponding to the ^{5}He ground state. We therefore concentrate on determination of the n+^{4}He potential using this resonance and

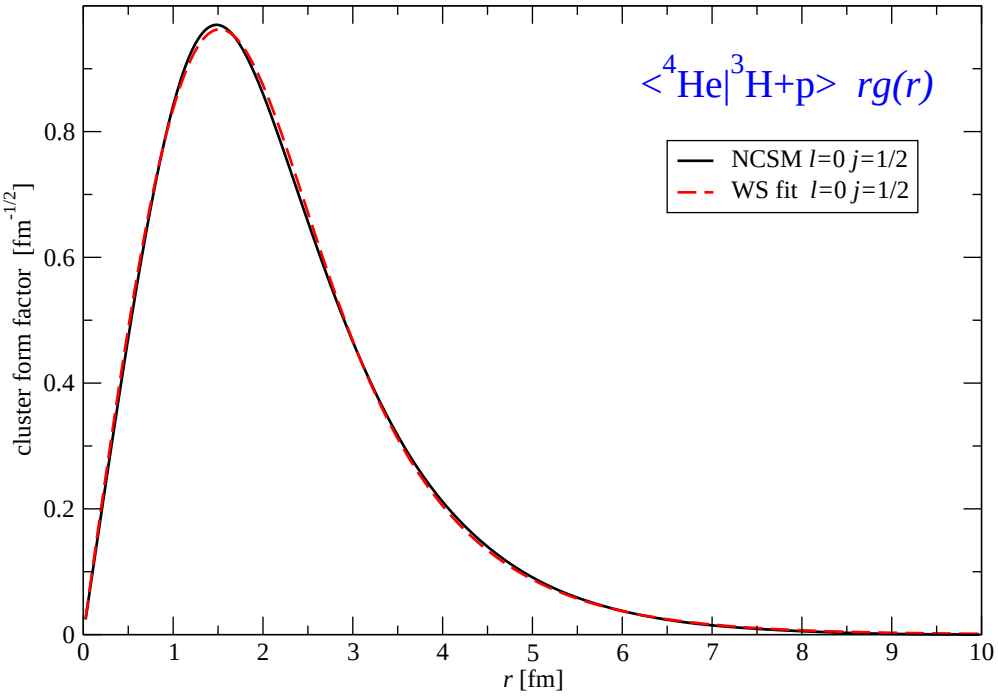

FIG. 9: Overlap function, $rg(r)$, for the ground state of ^{4}He with the ground state of ^{3}H plus proton as a dependence of their separation. The s-wave channel with $j = 1/2$ is shown. The full line represents the NCSM result obtained using the CD-Bonn 2000 NN potential, the $18\hbar\Omega$ model space and the HO frequency of $\hbar\Omega = 28$ MeV. The dashed lines represent corrected overlaps obtained from a Woods-Saxon potential whose parameters were fit to the NCSM overlap up to 6.0 fm under the constraint to reproduce the experimental separation energy.

subsequently we test whether the potential determined this way reproduces the $d3/2$ phase shift correctly.

In Fig. 10, we show by the solid black line the overlap function of ^{5}He with ^{4}He plus neutron obtained within the *ab initio* NCSM using the ^{5}He $3/2^-$ ground state wave function and the ^{4}He ground state wave function. In the same figure, we show by the red dashed line a resonance scattering wave function from WS potential fitted to the interior part of the *ab initio* overlap function at the experimental resonance energy of 0.89 MeV. During the fit, we kept the spin-orbit potential strength fixed at a value that we found to describe reasonably also the $p1/2$ channel. The WS parameters obtained in this fit are given in Table II.

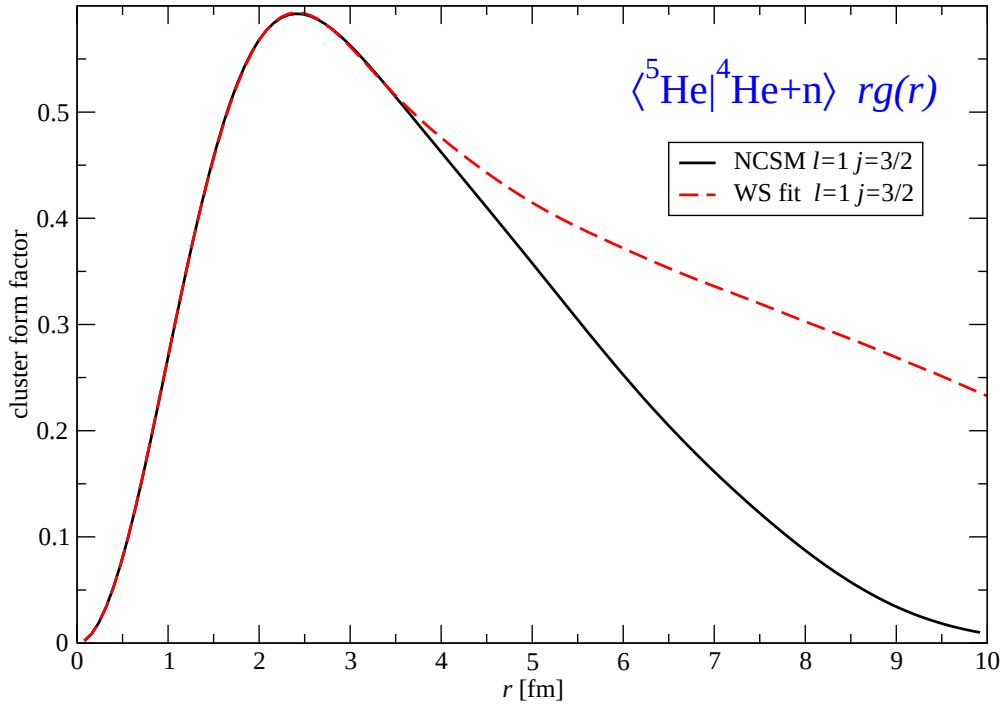

FIG. 10: Overlap function, $rg(r)$, for the ground state of ^{5}He with the ground state of ^{4}He plus neutron as a dependence of their separation. The p-wave channel with $j = 3/2$ is shown. The full line represents the NCSM result obtained using the CD-Bonn 2000 NN potential, the $12\hbar\Omega$ model space and the HO frequency of $\hbar\Omega = 16$ MeV. The dashed lines represent corrected overlaps obtained from a Woods-Saxon potential whose parameters were fit to the NCSM overlap up to 3.6 fm under the constraint to reproduce the experimental resonance energy of 0.89 MeV.

In Fig. 11, we present phase shift dependence on the center of mass energy of the n+^{4}He system for the $p3/2$, $p1/2$, $s1/2$ and $d3/2$ channels. The WS potential determined as described above and given in Table 2 was used. We repeat that the WS potential was determined from the ^{5}He $3/2^-$ resonance at a single energy corresponding to the experimental threshold energy. We can see that the potential not only describes rather well the $p3/2$ phase shifts in a very wide energy range from 0 up to about 20 MeV but it also describes reasonably phase shifts in other waves. We note that experimental data are displayed only for the $p3/2$ channel. The good behavior of the $d3/2$ phase shift is of particular importance as discussed earlier.

TABLE II: Parameters of the n+^{4}He Woods-Saxon potential obtained in the fit to the interior part of the NCSM ^{5}He $3/2^-$ resonance overlap function under the constraint to reproduce experimental threshold energy.

$\langle ^5\text{He}3/2^- \vert ^4\text{He+n}\rangle$					
V_0	R_0	a_0	V_{ls}	R_{ls}	a_{ls}
-65.162	1.762	0.510	-6.0	2.467	0.228

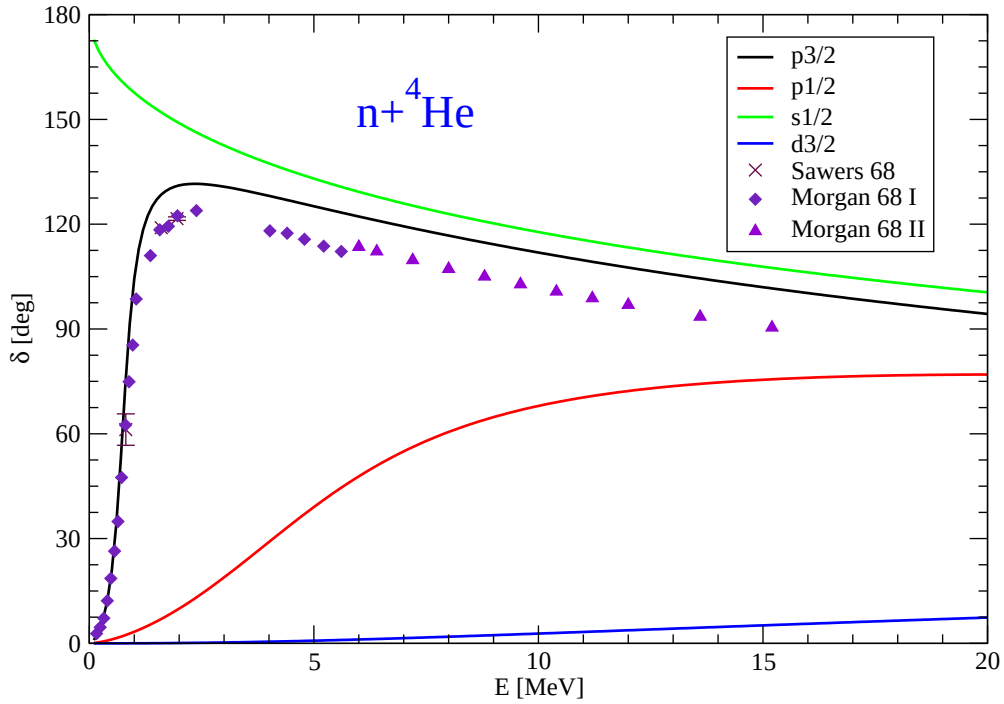

FIG. 11: The n+^{4}He phase shifts for the $p3/2$, $p1/2$, $s1/2$ and $d3/2$ channels in the 0 to 20 MeV center-of-mass energy range. Woods-Saxon potential obtained from the ^{5}He $3/2^-$ resonance overlap function fit shown in Fig. 10 was used for all channels. The experimental data are for the $p3/2$ channel.

C. ^{2}H+^{3}H scattering potential from the ^{5}He $3/2^+$ resonance *ab initio* wave function

The most challenging task is the determination of the d+t scattering potential. To determine this potential, we make use of the ^{5}He $3/2^+$ resonance known to play a pivotal

role in the ^{3}H(d,n)^{4}He transfer reaction. This resonance is dominated by the s-wave channel. However, due to the $J = 0$ spin of ^{4}He and $J = 1/2$ spin of the neutron, the outgoing n+^{4}He must be in a d wave. Consequently, tensor interaction plays a crucial role in the description of the transfer reaction. Therefore, we need to pay attention to the role of the tensor interaction not only in the deuteron bound state but also in the d+t $3/2^+$ resonant channel.

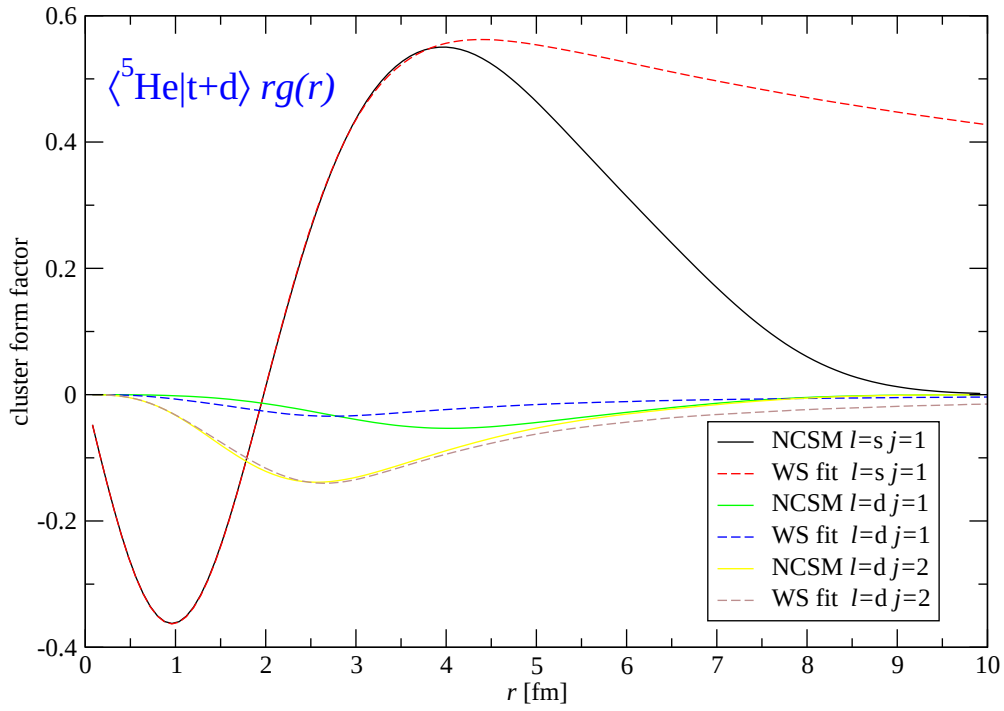

FIG. 12: Overlap functions, $rg(r)$, for the $3/2^+$ excited state of ^{5}He with the ground state of ^{3}H plus deuteron as a dependence of their separation. The s-wave channel with $j = 1$ abd d-wave channels with $j = 1, 2$ are shown. The full lines represent the NCSM results obtained using the CD-Bonn 2000 NN potential, the $12\hbar\Omega$ model space and the HO frequency of $\hbar\Omega = 13$ MeV. The dashed lines represent corrected overlaps obtained from a Woods-Saxon potential whose parameters were fit in a coupled channel calculation to all three shown NCSM overlaps simultaneously up to 4 fm under the constraint to reproduce the experimental resonance energy.

In Fig. 12, we present by full lines overlap functions of ^{5}He $3/2^+$ state with deuteron and ^{3}H obtained within the *ab initio* NCSM calculation. The ^{5}He $3/2^+$ state was actually the second excited $3/2^+$ state in our *ab initio* NCSM calculation. The first one has ba-

sically a zero overlap with the d+t and corresponds to a non-resonant n+^{4}He continuum state [7]. Unlike for the previously discussed overlap functions, there are three partial waves corresponding to the s wave with $j = 1$ and d waves with $j = 1$ and $j = 2$. The angular momentum j is coupled with the ^{3}H spin of 1/2 to the total $3/2^+$ resonance angular momentum. As emphasized above, the tensor interaction is crucial for understanding the ^{3}H(d,n)^{4}He transfer reaction. We must find a potential that couples all three partial waves. This potential should have a tensor, spin-spin and also spin-orbit component. To find such a potential, we wrote a new code named Pluto capable to solve coupled-channel equations for the d+t system. The code uses Lagrange-mesh method in combination with the microscopic R-matrix approach to solve the problem. The code is called by the separate least-square fitting code that determines the potential parameters. The result of our coupled-channel fit of the interior of the *ab initio* NCSM overlap functions is shown by dashed lines in Fig. 12. The fit was constrained to reproduce the experimental threshold energy. We can see that the two dominant overlap functions are fitted rather well. The relative sign of the partial waves plays a role in determination of the tensor and spin-orbit potentials. The WS parameters obtained in our fit are given in Table III.

TABLE III: Parameters of the d+t Woods-Saxon potentials obtained in the fits to the interior part of the NCSM ^{5}He $3/2^+$ resonance overlap functions under the constraint to reproduce experimental threshold energy. The V_0' in the last line is a modified central potential discussed in the text.

$\langle^5$He $3/2^+$|d+t$\rangle$					
V_0	R_0	a_0	$V_{\rm ls}$	$R_{\rm ls}$	$a_{\rm ls}$
-48.76	2.280	0.685	14.786	1.872	0.363
$V_{\rm ss}$	$R_{\rm ss}$	$a_{\rm ss}$	$V_{\rm T}$	$R_{\rm T}$	$a_{\rm T}$
-5.0	1.217	0.054	-2.354	1.983	0.434
V_0'	R_0'	a_0'			
-74.6	1.95	0.45			

D. ^{3}H(d,n)^{4}He S-factor from the combined *ab initio*/potential model approach

Using the potentials and spectroscopic factors obtained as described in previous subsections and summerized in Tables I, II and III, we performed coupled-channel calculations of the ^{3}H(d,n)^{4}He transfer reaction using the code Fresco. This does not include antisymmetrisation between the clusters, so that the reaction mechanism must be calculated by distinct contributions from proton and deuteron transfers. This is because the same final states can be reached by viewing the transfer as $(n+p)_d + t \rightarrow (t+p)_\alpha + n$ as well as $d + (d+n)_t \rightarrow (d+d)_\alpha + n$.

The transfer calculation uses a total system wave function of

$$\Psi^{JM} = \psi_d \psi_t \varphi^J_L(R_{dt}) + \psi_\alpha \psi_n \varphi^J_{L'}(R_{\alpha n}) \tag{15}$$

in which the ψ's are the bound states of the respective nuclei, and the φ_L are the scattering wave functions satisfying boundary conditions for $R_{dt}, R_{\alpha n} \gg R_m$ of

$$\begin{aligned} \varphi^J_L(R_{dt}) &= \frac{i}{2}[\delta_{LL_i} H^-_L(k_{dt}R_{dt}) - S^J_{LL_i} H^+_L(k_{dt}R_{dt})], \\ \varphi^J_{L'}(R_{\alpha n}) &= -\frac{i}{2} S^J_{L'L_i} H^+_{L'}(k_{\alpha n}R_{\alpha n}) \ . \end{aligned} \tag{16}$$

Here L_i is the partial wave with the component of the $d+t$ incoming plane wave.

The scattering wave functions $\varphi_L(R)$ are found by solving the standard coupled integro-differential equations

$$\begin{aligned} [T_{dt} + U_{dt} - E_{dt}]\varphi^J_L(R_{dt}) + \int_0^{R_m} V^J_{dt:\alpha n}(R_{dt}, R_{\alpha n})\varphi^J_{L'}(R_{\alpha n}) dR_{\alpha n} &= 0 \\ [T_{\alpha n} + U_{\alpha n} - E_{\alpha n}]\varphi^J_{L'}(R_{\alpha n}) + \int_0^{R_m} V^J_{\alpha n:dt}(R_{\alpha n}, R_{dt})\varphi^J_L(R_{dt}) dR_{dt} &= 0 \ . \end{aligned} \tag{17}$$

The channel potentials U_{dt} and $U_{\alpha n}$ are used from the above analyses of the NCSM resonance wave functions. The non-local transfer kernels are the sum of

$$V^{J;n}_{dt:\alpha n}(R_{dt}, R_{\alpha n}) = \langle [\psi_d \psi_t Y_L(\hat{R}_{dt})]_J | V_{pn} + V_{tn} - U_{\alpha n} | [\psi_\alpha \psi_n Y_{L'}(R_{\alpha n})]_J \rangle \ . \tag{18}$$

for the 'direct' neutron transfer $(n+p)_d + t \rightarrow (t+p)_\alpha + n$, and of

$$V^{J;d}_{dt:\alpha n}(R_{dt}, R_{\alpha n}) = \langle [\psi_d \psi_t Y_L(\hat{R}_{dt})]_J | V_{dn} + V_{dn} - U_{\alpha n} | [\psi_\alpha \psi_n Y_{L'}(R_{\alpha n})]_J \rangle \ . \tag{19}$$

for the 'exchange' deuteron transfer $d + (d+n)_t \rightarrow (d+d)_\alpha + n$.

When the direct and exchange transfer mechanisms both included, we obtain the S-factor presented in Fig. 13 by the dashed line together with the experimental data. We use a matching radius of $R_m = 15$ fm, as increasing this radius to 20 or 25 fm has negligible effect.

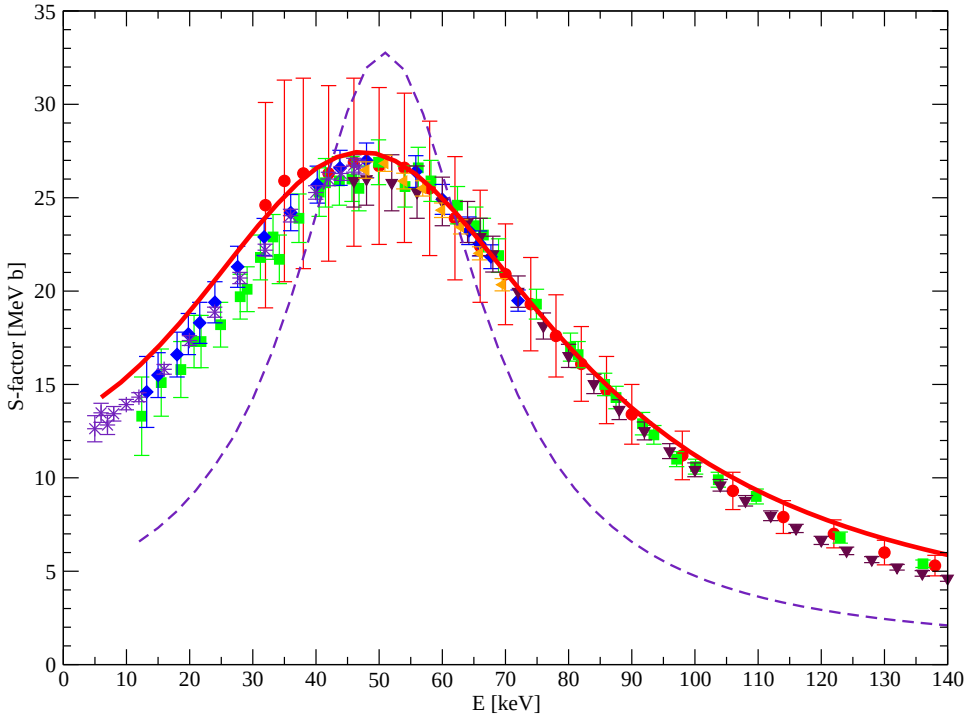

FIG. 13: S-factor of the ^{3}H(d,n)^{4}He transfer reaction calculated in the coupled channel formalism with cluster-cluster potentials obtained from the *ab initio* overlap function fits is compared to experimental data. The dashed line correspond to calculation with all parameters determined from *ab initio* NCSM overlap functions. The full line corresponds to calculation with re-adjusted d+t central potential parameters.

We can see that the theoretical calculation agrees with experiment within a factor of two. This is a significantly larger disagreement than we found for S-factors of capture reactions. It should be noted, however, that complexity of the ^{3}H(d,n)^{4}He S-factor calculation is far greater due to the importance of many channels, and the necessity to construct scattering potentials by fitting resonances in a coupled-channels approach. Further, the physical

model that we rely on lacks some important features, in particular the antisymmetrization of nucleons from different subclusters in the final Fresco calculation. This was not the case in the capture reaction calculations. In a fully antisymmetrised model, we would not separately calculated the contributions from proton and deuteron transfers, as both would be automatically included.

To improve agreement with experiment, we adjusted the radius and the diffusness of the central part of the d+t potential by about 20% and readjusted the central potential strength to fit the experimental position of the resonance. The modified parameters are shown in the last line of Table III. The S-factor result after this re-adjustment is presented in Fig. 13 by the full line. We can see an almost perfect agreement with the data. It should be emphasized that this kind of agreement would not be possible without the spin-orbit and in particular the tensor interaction in the d+t potential determined from our *ab initio* NCSM overlap functions. The modified radius and diffuseness of the central potential suggests a smaller radius of the ^{5}He $3/2^+$ state compared to that we obtained in our *ab initio* NCSM calculation. However, a typical problem with the *ab initio* NCSM is an *under*estimation of radii due to the use of the HO basis, i.e. incorrect description of the long-range correlations. Therefore, we believe that the need to re-adjust the radius of the central potential is a result of some other problem in the approach, such as the lack of inter-cluster antisymmetrization in the final coupled-channels calculation which requires the proton and deuteron transfer matrix elements to be calculated separately.

V. CONCLUSIONS

We presented coupled channel calculations of the S-factor of ^{3}H(d,n)^{4}He transfer reaction. Potentials of different subclusters relevant for description of the transfer reaction were obtained by fits to cluster overlap functions calculated within the *ab initio* no-core shell model. This type of combined *ab initio*/potential model approach was successfully applied in the past to describe low-energy capture reactions important for nuclear astrophysics. For those reactions, typically a single or just a few channels were needed for an accurate description of the S-factor. For the ^{3}H(d,n)^{4}He transfer reaction, many channels are relevant, which makes the application of the combined approach quite challenging. The result of our theoretical calculation with all parameters determined from the *ab initio* NCSM overap functions agrees

with experiment within a factor of two. By performing a simple re-adjustment of the order of 20% of d+t central potential radius and diffuseness parameters, we obtain an almost perfect agreement with the experimental data. This kind of agreement would not be possible without the spin-orbit and in particular the tensor interaction in the d+t potential determined from our *ab initio* NCSM overlap functions. The modified radius and diffuseness of the central potential suggests a smaller radius of the ^{5}He $3/2^+$ state compared to that we obtained in our *ab initio* NCSM calculation. However, it is known that the *ab initio* NCSM typically underestimates radii due to the use of the HO basis, i.e. incorrect description of the long-range correlations. Therefore, we believe that the need to re-adjust the radius of the central potential is a result of some other problem in the approach, such as the lack of inter-cluster antisymmetrization in the final coupled channel calculation.

VI. OUTLOOK: TOWARDS A FULLY *AB INITIO* CALCULATION OF THE ^{3}H(D,N)^{4}HE S-FACTOR

In the previous section, we highlighted shortcomings of the *ab initio* NCSM, its incorrect description of long-range correlations and its lack of coupling to continuum. Further, we highlighted a potential problem of the coupled-channel approach due to the neglect of the Pauli principle, i.e. the inter-cluster antisymmetrization.

If we want to build upon the *ab initio* NCSM to microscopically describe loosely bound systems as well as nuclear reactions, the approach must be augmented by explicitly including cluster states such as, e.g. those given in Eq. (1), and solve for their relative motion while imposing the proper boundary conditions. This can be done by extending the *ab initio* NCSM HO basis through the addition of the cluster states. This would result in an overcomplete basis with the cluster relative motion wave functions as amplitudes that need to be determined. The first step in this direction is to consider the cluster basis alone. This approach is very much in the spirit of the resonating group method (RGM) [24], a technique that considers clusters with fixed internal degrees of freedom, treats the Pauli principle exactly and solves the many-body problem by determining the relative motion between the various clusters. In our approach, we use the *ab initio* NCSM wave functions for the clusters involved and the *ab initio* NCSM effective interactions derived from realistic NN (and eventually also from NNN) potentials.

The general outline of the formalism is as follows. The many-body wave function is approximated by a superposition of binary cluster channel wave functions

$$\Psi^{(A)} = \sum_{\nu} \hat{\mathcal{A}} \left[\psi_{1\nu}^{(A-a)} \psi_{2\nu}^{(a)} \varphi_{\nu}(\vec{r}_{A-a,a}) \right] = \sum_{\nu} \int d\vec{r}\, \varphi_{\nu}(\vec{r})\, \hat{\mathcal{A}}\, \Phi_{\nu\vec{r}}^{(A-a,a)} \,, \tag{20}$$

with

$$\Phi_{\nu\vec{r}}^{(A-a,a)} = \psi_{1\nu}^{(A-a)} \psi_{2\nu}^{(a)} \delta(\vec{r} - \vec{r}_{A-a,a}) \,. \tag{21}$$

Here, $\hat{\mathcal{A}}$ is the antisymmetrizer accounting for the exchanges of nucleons between the two clusters (which are already antisymmetric with respect to exchanges of internal nucleons). The relative-motion wave functions φ_ν depend on the relative-distance between the center of masses of the two clusters in channel ν. They can be determined by solving the many-body Schrödinger equation in the Hilbert space spanned by the basis functions (21):

$$H\Psi^{(A)} = E\Psi^{(A)} \longrightarrow \sum_{\nu} \int d\vec{r} \left[\mathcal{H}_{\mu\nu}^{(A-a,a)}(\vec{r}\,', \vec{r}) - E\mathcal{N}_{\mu\nu}^{(A-a,a)}(\vec{r}\,', \vec{r}) \right] \varphi_{\nu}(\vec{r}) \,, \tag{22}$$

where the Hamiltonian and norm kernels are defined as

$$\mathcal{H}_{\mu\nu}^{(A-a,a)}(\vec{r}\,', \vec{r}) \;=\; \left\langle \Phi_{\mu\vec{r}\,'}^{(A-a,a)} \left| \hat{\mathcal{A}}\, H\, \hat{\mathcal{A}} \right| \Phi_{\nu\vec{r}}^{(A-a,a)} \right\rangle \,, \tag{23}$$

$$\mathcal{N}_{\mu\nu}^{(A-a,a)}(\vec{r}\,', \vec{r}) \;=\; \left\langle \Phi_{\mu\vec{r}\,'}^{(A-a,a)} \left| \hat{\mathcal{A}}^2 \right| \Phi_{\nu\vec{r}}^{(A-a,a)} \right\rangle \,. \tag{24}$$

The most challenging task is to evaluate the Hamiltonian kernel and the norm kernel. We now briefly outline, how this is done when *ab initio* NCSM wave functions are used for the binary cluster states. From now on, let us consider the cluster states with a single-nucleon projectile ($a = 1$ in Eq. 20). A generalization is straightforward. Using an alternative coupling scheme compared to Eq. (1), we introduce

$$\begin{aligned} & \langle \vec{\xi}_1 \ldots \vec{\xi}_{A-2} \xi'_{A-1} \hat{\xi}_{A-1} | \Phi^{(A-1,1)JMTM_T}_{(\alpha I_1 T_1, \frac{1}{2}\frac{1}{2});sl}; \delta_{\xi_{A-1}} \rangle \\ =\; & \sum (I_1 M_1 \tfrac{1}{2} m_s | sm)(sml m_l | JM)(T_1 M_{T_1} \tfrac{1}{2} m_t | TM_T) \frac{\delta(\xi_{A-1} - \xi'_{A-1})}{\xi_{A-1}\xi'_{A-1}} \\ \times\; & Y_{lm_l}(\hat{\xi}_{A-1}) \chi_{m_s} \chi_{m_t} \langle \vec{\xi}_1 \ldots \vec{\xi}_{A-2} | A-1 \alpha I_1 M_1 T_1 M_{T_1} \rangle \,, \end{aligned} \tag{25}$$

with the spin and isospin coordinates omitted to simplify the notation. The Jacobi coordinates were defined in Eq. (2). Using the latter cluster basis and the following definition of the antisymmetrizer $\hat{\mathcal{A}} = 1/\sqrt{A}(1 - \sum_{j=1}^{A-1} P_{j,A})$ with $P_{j,A}$ the transposition operator of nucleons j and A, the norm kernel can be expressed as

$$\begin{aligned} \mathcal{N}_{\mu\nu}^{(A-1,1)}(r', r) \;=\; & \delta_{\mu\nu} \frac{\delta(r'-r)}{r'r} - (A-1) \sum_{n'n} R_{n'l'}(r') \\ & \times\; \langle \Phi^{(A-1,1)JT}_{(\alpha' I'_1 T'_1, \frac{1}{2}\frac{1}{2})s'l'}; n'l' | P_{A,A-1} | \Phi^{(A-1,1)JT}_{(\alpha I_1 T_1, \frac{1}{2}\frac{1}{2})sl}; nl \rangle R_{nl}(r) \,, \end{aligned} \tag{26}$$

with $\mu \equiv (\alpha' I_1' T_1', \frac{1}{2}\frac{1}{2}) s'$, $\nu \equiv (\alpha I_1 T_1, \frac{1}{2}\frac{1}{2}) s$ and $P_{A,A-1}$ the transposition operator of nucleons A and $A-1$. The coordinates r are related to ξ_{A-1} by $r = \sqrt{\frac{A}{A-1}}\xi_{A-1}$ and the HO length parameter of the radial HO wave functions is $b = \sqrt{\frac{\hbar}{\frac{A-1}{A} m\Omega}}$. The matrix element of the transposition operator $P_{A,A-1}$ can be directly evaluated using the *ab initio* NCSM wave functions expanded in Jacobi coordinate HO basis. However, a crucial feature of the *ab initio* NCSM approach is that the matrix elements that enter the norm kernel and the Hamiltonian kernel can be equivalently evaluated using the *ab initio* NCSM wave functions expanded in the Slater determinant HO basis. This is achieved in two stages. First, we calculate the SD matrix element as

$$
\begin{aligned}
&{}_{\rm SD}\langle \Phi^{(A-1,1)JT}_{(\alpha' I_1' T_1', \frac{1}{2}\frac{1}{2}) s' l'}; n'l' | P_{A,A-1} | \Phi^{(A-1,1)JT}_{(\alpha I_1 T_1, \frac{1}{2}\frac{1}{2}) s l}; nl \rangle_{\rm SD} = \\
&\frac{1}{A-1} \sum_{jj'K\tau} \left\{ \begin{array}{ccc} I_1 & \frac{1}{2} & s \\ l & J & j \end{array} \right\} \left\{ \begin{array}{ccc} I_1' & \frac{1}{2} & s' \\ l' & J & j' \end{array} \right\} \left\{ \begin{array}{ccc} I_1 & K & I_1' \\ j' & J & j \end{array} \right\} \left\{ \begin{array}{ccc} T_1 & \tau & T_1' \\ \frac{1}{2} & T & \frac{1}{2} \end{array} \right\} \\
\times\ & \hat{s}\hat{s}'\hat{j}\hat{j}'\hat{K}\hat{\tau}(-1)^{I_1'+j'+J}(-1)^{T_1+\frac{1}{2}+T} \\
\times\ & {}_{\rm SD}\langle A-1 \alpha' I_1' T_1' || | (a^\dagger_{nlj\frac{1}{2}} \tilde{a}_{n'l'j'\frac{1}{2}})^{(K\tau)} | | | A-1 \alpha I_1 T_1 \rangle_{\rm SD} \, .
\end{aligned}
\tag{27}
$$

Second, it is possible to show that the matrix element in the SD basis is related to the one in the Jacobi coordinate basis:

$$
\begin{aligned}
&{}_{\rm SD}\langle \Phi^{(A-1,1)JT}_{(\alpha' I_1' T_1', \frac{1}{2}\frac{1}{2}) s' l'}; n'l' | P_{A,A-1} | \Phi^{(A-1,1)JT}_{(\alpha I_1 T_1, \frac{1}{2}\frac{1}{2}) s l}; nl \rangle_{\rm SD} = \\
&\sum_{n_r l_r n_r' l_r' J_r} \langle \Phi^{(A-1,1)J_r T}_{(\alpha' I_1' T_1', \frac{1}{2}\frac{1}{2}) s' l_r'}; n_r' l_r' | P_{A,A-1} | \Phi^{(A-1,1)J_r T}_{(\alpha I_1 T_1, \frac{1}{2}\frac{1}{2}) s l_r}; n_r l_r \rangle \\
\times\ & \sum_{NL} \hat{l}\hat{l}' \hat{J}_r^2 (-1)^{s+l_r-s-l_r'} \left\{ \begin{array}{ccc} s & l_r & J_r \\ L & J & l \end{array} \right\} \left\{ \begin{array}{ccc} s' & l_r' & J_r \\ L & J & l' \end{array} \right\} \\
\times\ & \langle n_r l_r NL l | 00 nll \rangle_{\frac{1}{A-1}} \langle n_r' l_r' NL l' | 00 n' l' l' \rangle_{\frac{1}{A-1}} \, .
\end{aligned}
\tag{28}
$$

This relation then defines a matrix that one inverts to get the Jacobi-coordinate matrix element. This is analogous to what was done to obtain the translationally invariant density in Ref. [25]. The Hamiltonian kernel can be evaluated in a similar yet more involved way. It consists of a kinetic term, a NN potential direct term associated with the operator $V_{A,A-1}(1-P_{A,A-1})$ and a NN potential exchange term associated with the operator $V_{A,A-2}P_{A,A-1}$ (plus terms arising from the NNN interaction). The ability to employ wave functions expanded in the SD basis opens the possibility to apply this formalism for nuclei with $A > 5$.

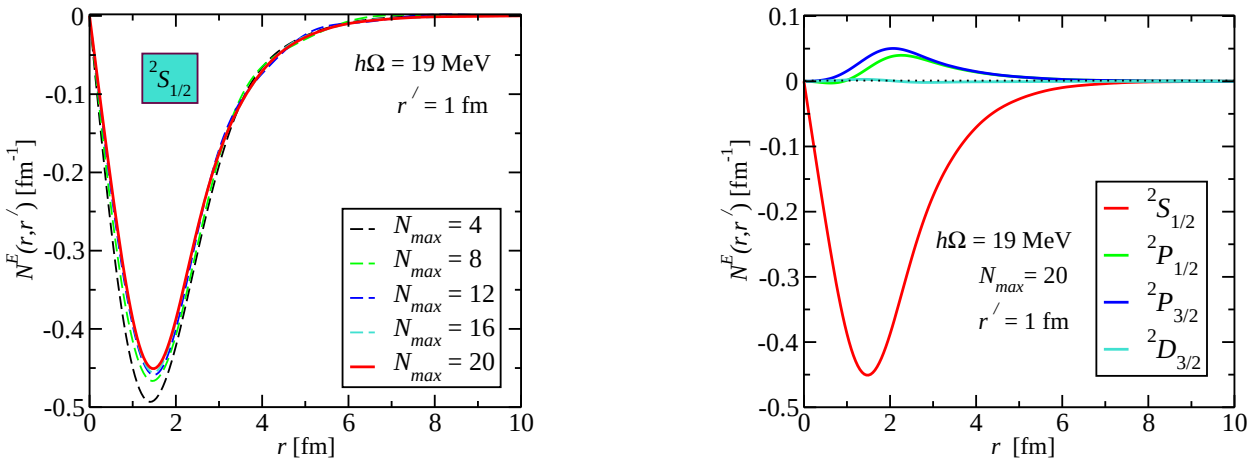

FIG. 14: The exchange part of the norm kernel of the n+^{4}He system. Left, the convergence with the size of the basis of the ^{4}He wave function for the $^2S_{1/2}$ channel. Right, results for channels are compared. The chiral EFT NN potential was used.

In Fig. 14, we show the exchange part of the norm kernel for the n+^{4}He system, in particular the second term of Eq. (26) multiplied by rr'. It is apparent that we are able to reach convergence for the kernel. Furthemore, the $^2S_{1/2}$ channel shows, as it should the effect of the Pauli principle. Indeed, the ^{4}He wave function is dominated by the four nucleon s-shell configuration. The Pauli principle prevents adding the fifth nucleon to the same shell.

In Fig. 15, we show the direct and the exchange contributions of the NN potential to the Hamiltonian kernel as well as their sum for the n+^{4}He system. Again, the Pauli principle is manifest in the $^2S_{1/2}$ channel. We were able to obtain the presented results using wave functions expanded both in the Jacobi-coordinate and the SD basis. The two independent calculations gave identical results as expected. Full details regarding this approach will be given in Ref. [26]. Here, we present preliminary n+^{4}He phase shift result for the $^2S_{1/2}$, $^2P_{3/2}$, $^2P_{1/2}$ and $^2D_{3/2}$ channels in Fig. 16. The results obtained so far are quite sensible and promising. For a comparison, see Fig. 11 with the phase shifts obtained using our fitted WS potential. We are able to reach convergence with realistic low-momentum V$_{\mathrm{low}k}$ NN interactions [27]. We are confident that using the combined NCSM-RGM approach is the right way to calculate the ^{3}H(d,n)^{4}He S-factor from first pinciples and with a predictive power.

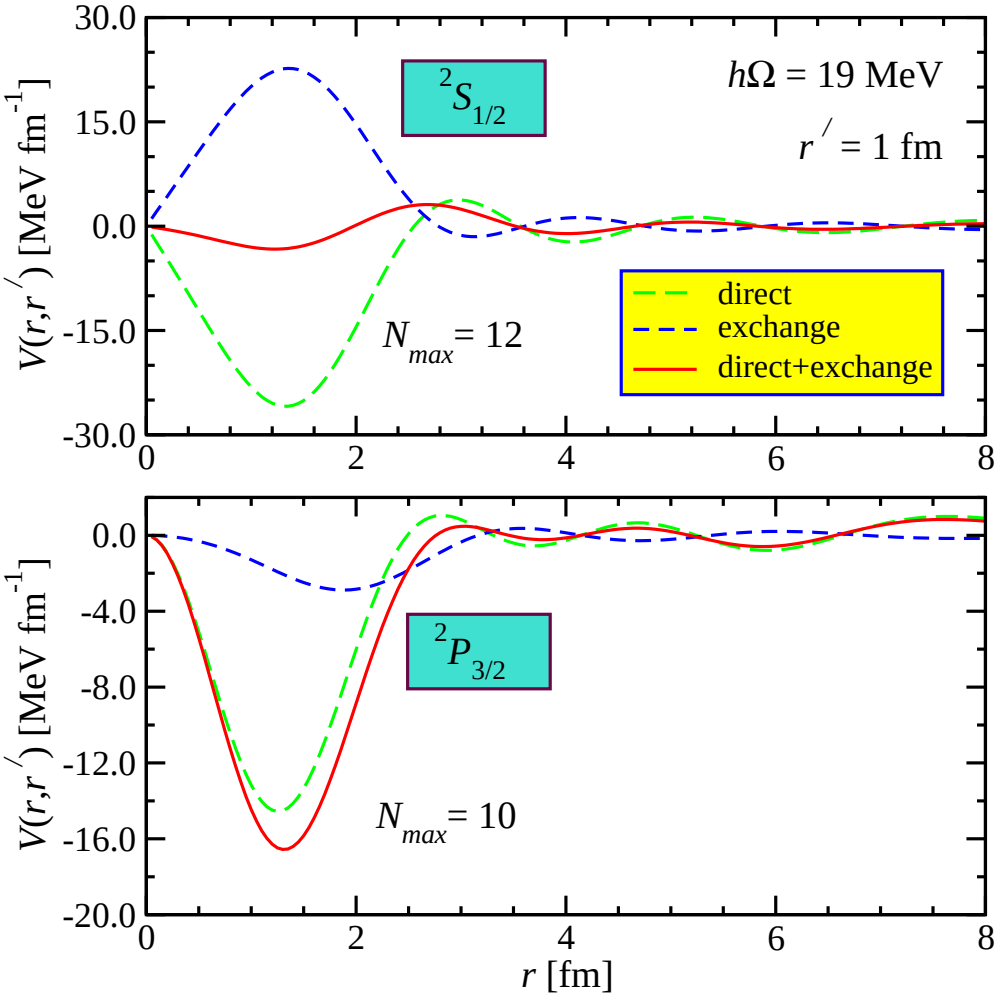

FIG. 15: The NN potential direct and exchange terms of the Hamiltonian kernel of the n+^{4}He system. The $^2S_{1/2}$ and $^2P_{3/2}$ channels are compared. The chiral EFT NN potential was used.

Acknowledgments

This work was performed under the auspices of the U. S. Department of Energy by the University of California, Lawrence Livermore National Laboratory under contract No. W-7405-Eng-48.

[1] J. Hale, private communication

[2] P. Navrátil, J. P. Vary and B. R. Barrett, Phys. Rev. Lett. **84**, 5728 (2000); Phys. Rev. C **62**,

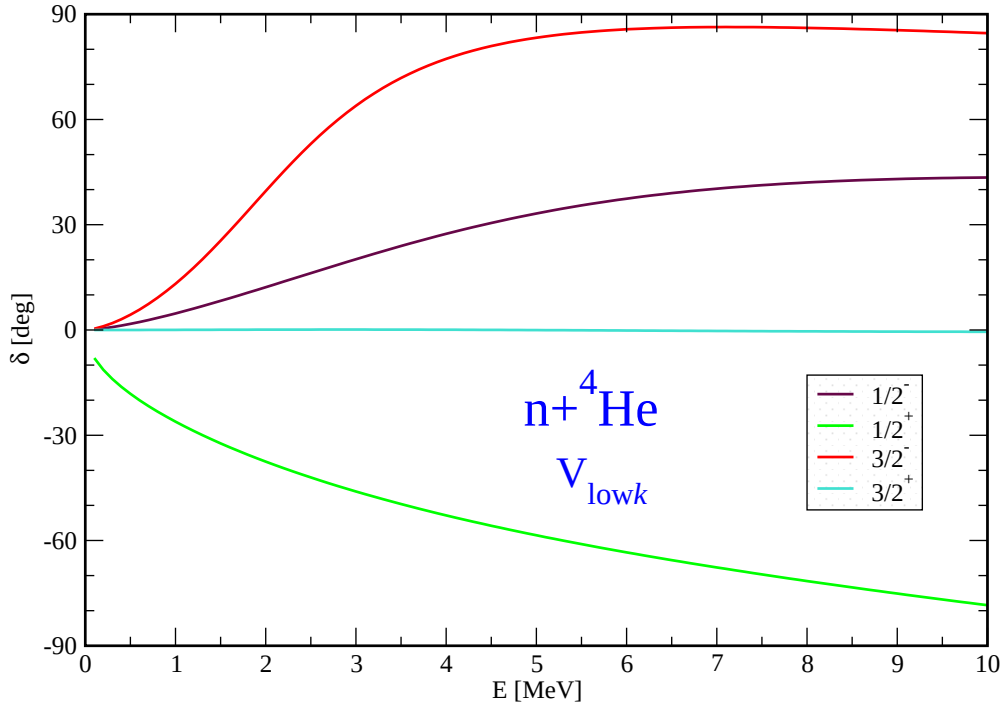

FIG. 16: The phase shifts of the n+^{4}He system obtained in a fully *ab initio* calculation with no adjustable parameters. Results of a converged calculation using the low-momentum $V_{low k}$ NN interaction are presented.

054311 (2000).

[3] P. Navrátil, G. P. Kamuntavičius and B. R. Barrett, Phys. Rev. C **61**, 044001 (2000).

[4] P. Navrátil and W. E. Ormand, Phys. Rev. C **68**, 034305 (2003).

[5] K. Suzuki and S. Y. Lee, Prog. Theor. Phys. **64**, 2091 (1980).

[6] K. Suzuki and R. Okamoto, Prog. Theor. Phys. **92**, 1045 (1994).

[7] P. Navrátil, Phys. Rev. C **70**, 054324 (2004).

[8] R. Machleidt, Phys. Rev. C **63**, 024001 (2001).

[9] E. Adelberger *et al.*, Rev. Mod. Phys. **70**, 1265 (1998).

[10] SNO Collaboration, S. N. Ahmed *et al.*, Phys. Rev. Lett. **92**, 181301 (2004).

[11] S. Couvidat, S. Turck-Chièze, and A. G. Kosovichev, Astrophys. J. **599**, 1434 (2003).

[12] J. N. Bahcall and M. H. Pinsonneault, Phys. Rev. Lett. **92**, 121301 (2004).

[13] B. W. Filippone, A. J. Elwyn, C. N. Davids, and D. D. Koetke, Phys. Rev. Lett **50**, 412 (1983); Phys. Rev. C **28**, 2222 (1983).

[14] P. Navrátil, C. A. Bertulani and E. Caurier, Phys. Lett. B **634**, 191 (2006).

[15] P. Navrátil, C. A. Bertulani and E. Caurier, Phys. Rev. C **73**, 065801 (2006).

[16] H. Esbensen and G. F. Bertsch, Nucl. Phys. **A 600**, 37 (1996).

[17] R. G. H. Robertson, Phys. Rev. C **7**, 543 (1973).

[18] A. R. Junghans, E. C. Mohrmann, K. A. Snover, T. D. Steiger, E. G. Adelberger, J. M. Casandjian, H. E. Swanson, L. Buchmann, S. H. Park, A. Zyuzin, and A. M. Laird, Phys. Rev. C **68**, 065803 (2003).

[19] N. Iwasa *et al.*, Phys. Rev. Lett. **83**, 2910 (1999); B. Davids *et al.*, Phys. Rev. Lett. **86**, 2750 (2001); F. Schümann *et al.*, Phys. Rev. Lett. **90**, 232501 (2003).

[20] B. T. Kim, T. Izumuto and K. Nagatani, Phys. Rev. C **23**, 33 (1981).

[21] K. M. Nollett, Phys. Rev. C **63**, 054002 (2001)

[22] C. R. Brune, R. W. Kavanagh and C. Rolfs, Phys. Rev. C **50**, 2205 (1994).

[23] P. Navrátil, C. A. Bertulani and E. Caurier, Nucl. Phys. **A787**, 539c (2007).

[24] Y. C. Tang, M. LeMere and D. R. Thompson, Phys. Rep. **47** 167 (1978); K. Langanke and H. Friedrich, *Advances in Nuclear Physics*, chapter 4., Plenum, New York, 1987; R. G. Lovas, R. J. Liotta, A. Insolia, K. Varga and D. S. Delion, Phys. Rep. **294**, 265 (1998).

[25] P. Navrátil, Phys. Rev. C **70**, 014317 (2004).

[26] S. Quaglioni and P. Navrátil, to be published.

[27] S.K. Bogner, T. T. S. Kuo, and A. Schwenk, Phys. Rept. **386**, 1 (2003).